American Journal of Applied Sciences and Engineering (AJASE) | **ISSN** *2766-7596*
Published by ACADEMIC INK REVIEW | *https://airjournal.org/ajase*
12011 WestBrae Pkwy, Houston, TX 77031, United States
airjournals@gmail.com; enquiry@airjournal.org

Experimental Correlation between Heat Treatment Parameter and Corrosion Behavior of 800 Series Ni-Fe Superalloy in H_2SO_4 Solution

C.C. Nwogbu[1], P.I. Nwogbu[2], M.O. Arum[3]
[1]Depatment of Metallurgical and Materials Engineering
Enugu State University of Science and Technology, Enugu, Nigeria
[2&3]Department of Chemical Engineering
Enugu State University of Science and Technology, Enugu, Nigeria

Publication Process	*Date*
Received	***May 7th 2021***
Accepted	***May 15th 2021***
Published	***May 31st 2021***

ABSTRACT

This experiment was carried out to investigate the correlation between heat treatment parameter and corrosion behavior of incoloy 800 super-alloy in H2SO4 solution. Spark plasma sintering (SPS) was used in producing the samples. The produced samples were heat treated at temperatures of 800°c and 10000c and for of 1 and 2 hours at each temperature. Electrochemical studies were carried out in H2SO4 medium, using potentiodynammic anodic polarization techniques. From the results obtained, the heat-treated alloy showed better corrosion resistance than the untreated alloy. Heat treatment temperature and time have great influences on the corrosion behavior and morphology of the alloy. The sample heat treated at 1000°C for 1hour gave a high protection efficiency of 86.29%. It has been established from the result of the experiment that heat treatment can be used to improve the corrosion resistance of the alloy.

Keywords: *Ni-FE alloy, Microstructure, Corrosion, acid medium and Heat Treatment*

Introduction

Nickel-Iron base super-alloys possess higher tolerance for alloying elements in solid solution than stainless steels and other iron base alloys [Wlodek, Kelly, & Alden, 1992]. In addition, the good metallurgical stability of the nickel base alloys makes them a better alternative to stainless steel [Soucail, Marty, & Octor, 1996]. These alloys appear to be a promising alternative to austenitic stainless steels because of their better corrosion resistance, thermal conductivity and mechanical properties. Using these alloys, complex processes and waste streams can be handled safely due to their high corrosion resistance [Viswanathan, et. al., 2005; Locq, et. al., 2000]. Owing to the excellent mechanical and physical properties, nickel base super-alloys are extensively employed in nuclear power plants [Wesley & Copson, 1949].

Austenitic super-alloy, Incoloy 800 and 800H has the same basic composition (Fe–20Cr–32Ni) but with slight modification in 800H to control the carbon content (0.05-0.10 w%) and grain size [Singh & Sidhu, 2013]. The 800-nickel base solid solution strengthened super-alloy with major elemental composition as Ni-Fe-Cr, is a non-agnetic corrosion and oxidation resistant alloy. The major constituent elements nickel and chromium provide good resistance to oxidizing environments. In nuclear power plants, incoloy 800 is used as steam generator tubes [Dehmolaei, Shamanian, & Kermanpur, 2009]. This is as a result of its good mechanical strength, thermal conductivity, high formability and corrosion resistance.

Singh et al evaluated the high temperature performance of Ni-based superalloy Superni-75 under cyclic conditions for 1,000h in real service environment of the waste incinerator based upon medical waste as fuel. The performance has been characterized via surface morphology, phase composition and element concentration using the combined techniques of XRD, SEM/EDX, BSEI and EPMA. They reported that initially, due to chlorine-based corrosion attack on the Superni-75 alloy, there was inner penetration of the corrosive species. However, with the growth of a thin Cr2O3 interface layer along the scale/surface boundary, the performance of the alloy improved against the attack by the flue gases in the real service conditions of the medical waste incinerator. Boiler tubes made of Superni-75 were estimated to have an erosion-corrosion rate of about 65mils/year [Dehmolaei, Shamanian, & Kermanpur, 2009].

Paula Rojas [9] reported on the electrochemical behavior and corrosion resistance of glassy Fe68.6-Ni28.2-Mn3.2 (at%) specimens which were studied in different concentrations of acid solutions. The results indicated that the corrosion rate increased with increasing concentration of the acid solutions. Electrochemical impedance spectroscopy results were analyzed by fitting the experimental data to an equivalent circuit using the ZSim Demo program, and suitable equivalent circuit models were determined. The results obtained from the impedance and polarization measurements are in good agreement. The thermodynamic parameters were evaluated for the corrosion process and discussed. In order to further research in this novel area for better service condition, the present work has been undertaken.

Methodology

The alloy samples were produced using a spark plasma sintering machine (model SPS 10-3), manufactured by Thermal Technologies LLC. Specimens of diameter 100 mm were produced using dies and punches of graphite. The samples were produced at a temperature of 1150°C temperature and a pressure of 5MPa with heating and cooling rate of 10°C/Min. The thermocouple inserted into the bottom punch was used to measure the temperature. All the samples were produced in a closed furnace where 10-2 torr vacuum was maintained throughout the experiment. A standard Ni-Fe base super-alloy (Incoloy 800) with composition shown in Table 1a below was used for the experiment.

Table 1: Composition of the super-alloy incoloy 800 used

Ni	Fe	Cr	Mo	Mn	Si	C	Al	Ti	Cu	other
32.5	44.5	21	-	0.8	0.5	0.05	0.4	0.4	0.4	

The samples were heat treated using a carbolite furnace. The samples were placed inside the furnace and the following heat treatment program was used.

i. Hold at 1000°C for 1 and 2 hours: then rapidly cool by quenching in water.

ii. Hold at 800°C for 1 and 2 hours; then air cool,

X-ray diffraction (XRD) analysis, with Cu-Kα radiation, was conducted using a PANalytical X'Pert PRO. The XRD was operated at 45KV voltage and 40mA current.

The 2θ angles between 1° and 90° were scanned and analyzed using the Bragg Law. TOPASTM was used for quantitative analysis while TESCAN Scanning Electron Microscope was used in the research. The polished and etched samples were firmly held in the sample holder using a double-sided carbon tape before putting them inside the sample chamber. The SEM was operated at an accelerating voltage of 20 KV.

Electrochemical measurements were carried out using an Autolab potentiostat with the General-purpose Electrochemical Software package. The samples were cold mounted with epoxy leaving a working surface was ground with grinding papers from 600 to 1000 grit, and then cleaned with the distilled water and ethanol. A conventional three electrode cell, consisting of Ag/AgCl, Platinum and samples was used as: reference, counter and working electrodes respectively. The medium used for the electrochemical measurement was 0.5MHCl. The measurement was carried out at room temperature. The potentiodynamic potential scan was fixed from -1.5 V to +1.5 V with a scan rate of 0.012 V/s.

Results and Discussion

Figure 1a shows the XRD pattern of the untreated alloy, while Figures 1b-1e display the XRD patterns of the heat-treated samples. From the XRD spectrum of the alloy, it is observed clearly that there is presence of Ni, Fe (Awaruite), AL0.3Fe3 Si0.7 (Aluminum iron Silicon), and Cr7C3 (carbon Chromium) phases. After heat treatment it is observed that new phases appeared such as: FeSi (Fersilicite, syn [NR]), Managnese Carbide, Chromium Iron Carbide, Managanese Silicon Carbide. The presence of (Ni, Fe) (Awaruite) phase is common to all the samples; this expected because the specimen is a Ni-Fe base super-alloy. By comparing the XRD of the control (Figure 1a) with the heat-treated samples (Figures 1b- 1c), one can observe that there is a great change in the spectrum which resulted in more diffraction peaks, and a larger quantity of hard carbides with smaller inter-particle distance. In the heat-treated samples, it is clear that the various phases formed after the heat treatment depends on the heat treatment condition as shown in Table 2.

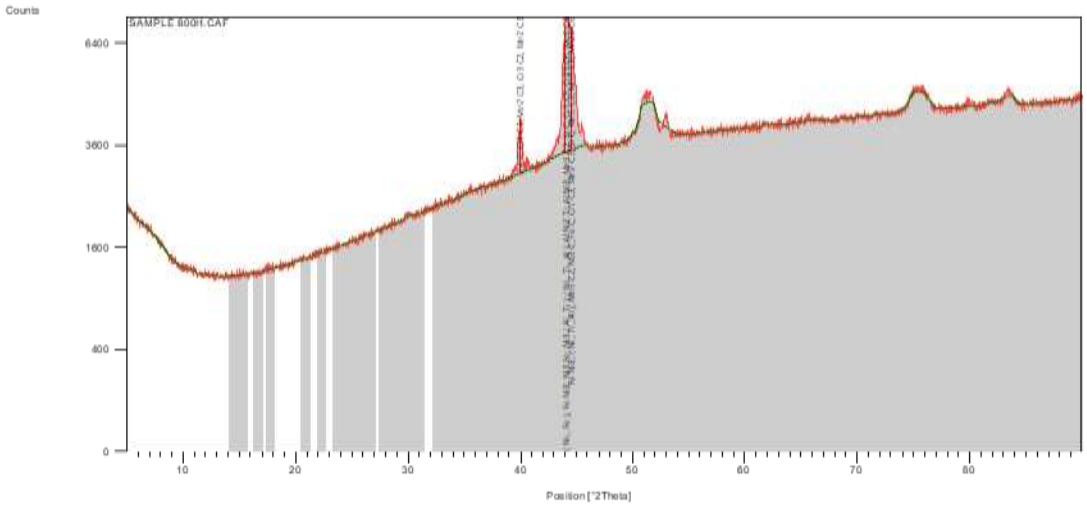

Figure 1a: XRD spectrum of untreated alloy

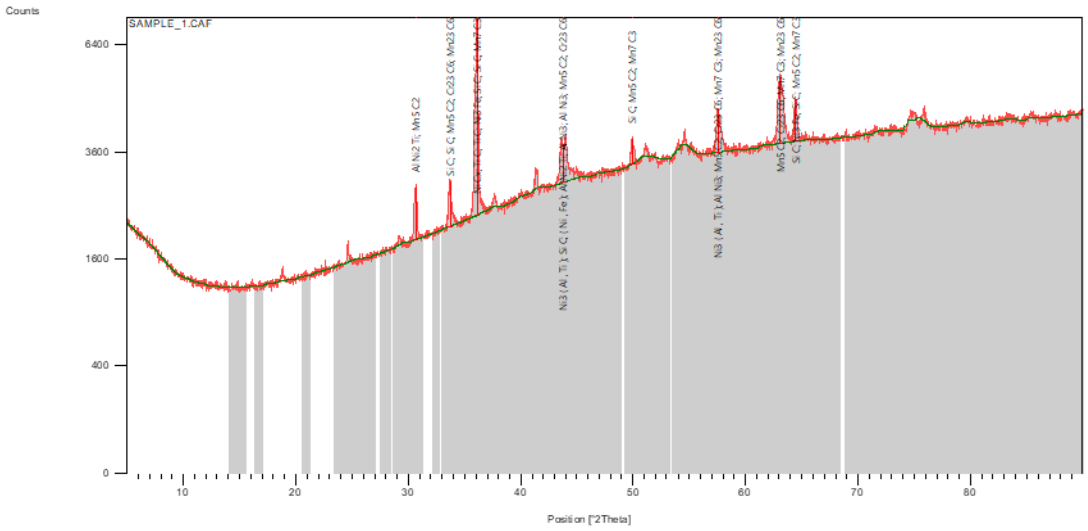

Figure 1b: XRD spectrum of Incoloy 800 alloy HT1000°C for 1hr

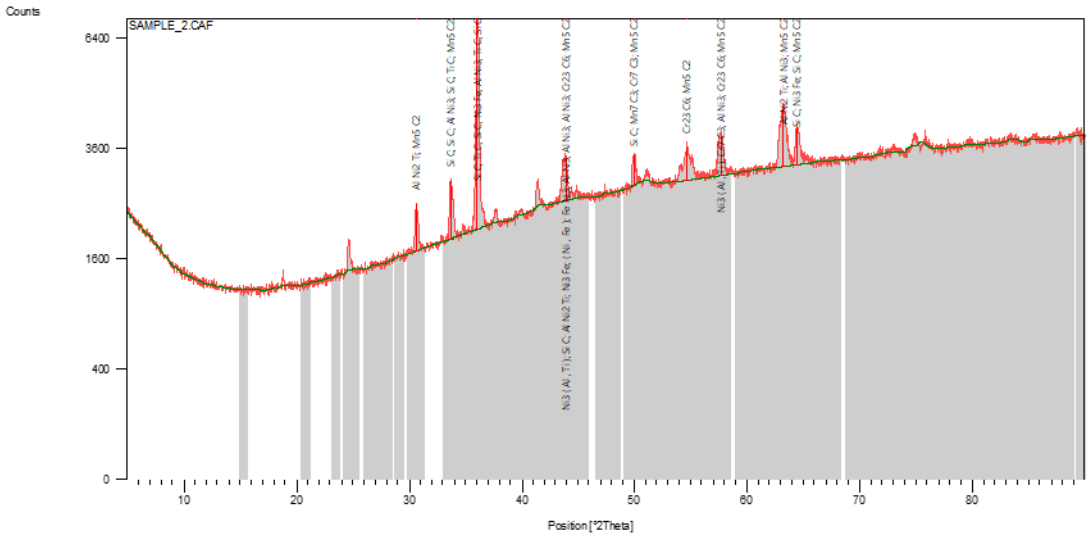

Figure 1c: XRD spectrum of Incoloy 800 alloy HT1000°C for 2hrs

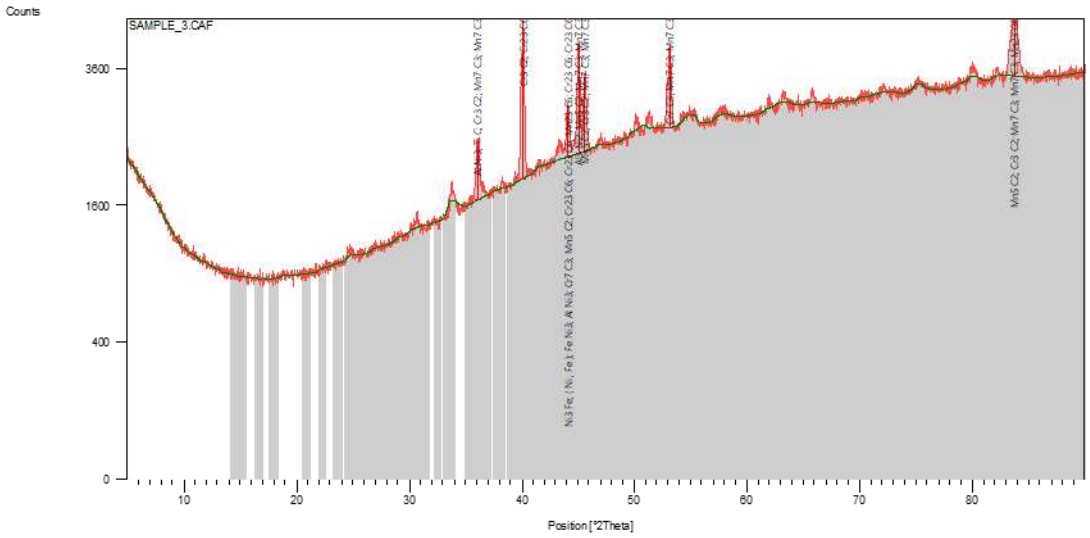

Figure 1d: XRD spectrum of Incoloy 800 alloy HT800°C for 1hr

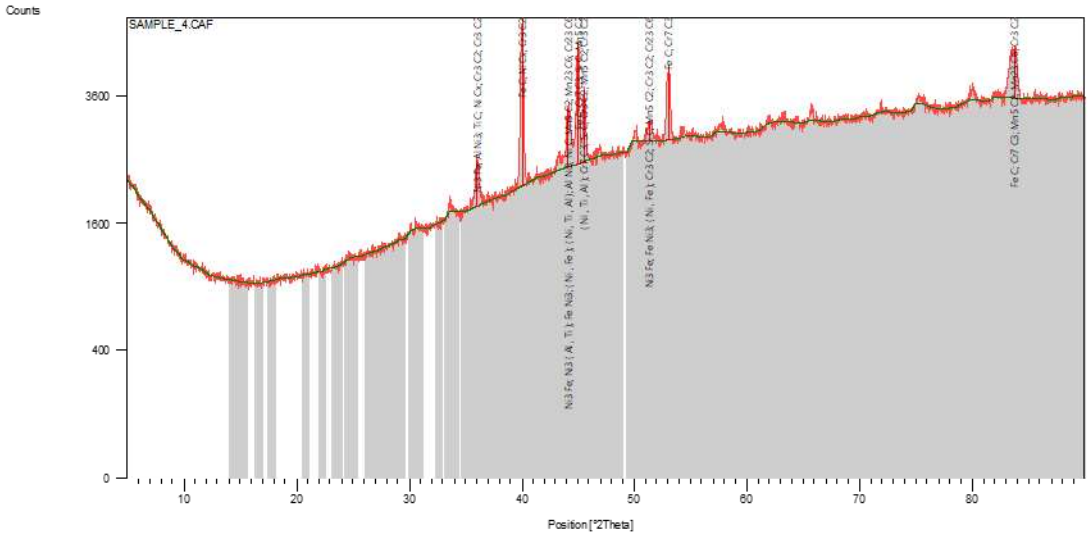

Figure 1e: XRD spectrum of Incoloy 800 alloy HT800°C for 2hrs

Discussion of Result

Table 2: Identified patterns list

Control	HT10001HR	HT10002HR	HT8001HR	HT8002HR
` (Ni, Fe) (Awaruite)	(Ni,Fe) (Awaruite)	Ni,Fe) Awaruite)	Ni,Fe) Awaruite)	Al Cr Fe2
Al0.3 Fe3 Si0.7 (Aluminum Iron Silicon)	Mn5 c2 (Manganese Carbide)	Al Ni2 Ti (Aluminum Nickel Titanium	Fe Si(Fersilicite, syn [NR])	Fe Si(Fersilicitie, syn [Nr])
Cr7C3 (Carbon Chromium)	Al0.5 Fe0.5 (Aluminum Iron)	Al0.96 Ni1.04 (Aluminum Nickel)	C0.12 Fe0.79 Si0.09 (Carbon Iron Silicon)	Fe Ni3 (Awaruite)
Ni3 (Al, Ti) (Udimet 500')	Mn Si (Manganese Silicon)	Fe7 C3 (Iron Cabide)	Fe3 C (Cementite)	Ni2 Si (Nickel Silicon)
	(Cr, Fe)7 C3 Chromium iron Carbide)	Al0.4 Fe0.6 (Aluminum Iron)	Cr3 Ni2 (Chromium Nickel)	Mn 15C4 (Manganese Carbide)
	Ni2.67 Ti1.33 (Nickel Titanium)	Cr22 C6 (Carbon Chromium)	Al2 Ti (Aluminum Titanium)	(Cr, Fe)7 C3 (Chromium Iron Carbide)
	Mn22.6 Si5.4 C4 (Manganese Silicon Carbide)		Ni74 Si26 (Nickel Silicon)	

From the Figures 2a-2e, one can observe a great difference between the morphology of the untreated alloy (see figure 2a) and those of the heat-treated samples (see figures 2b-2e). Sample heat treated for 1 hr. has a more refined structure. The dark spots show the presence of some of the new phases developed during heat treatment.

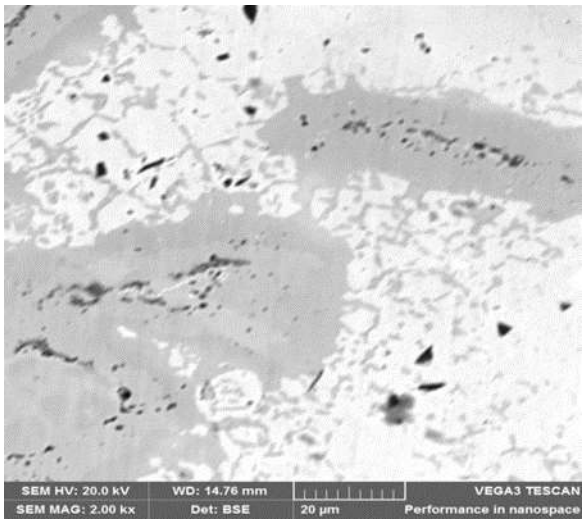

Figure2a: SEM image of untreated alloy

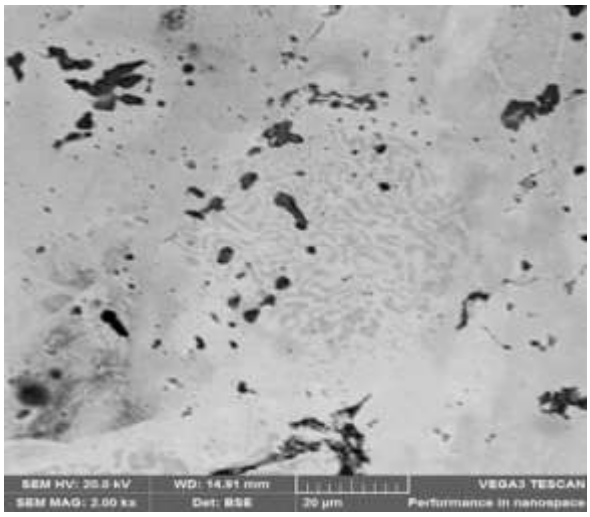

Figure2b: SEM image of alloy HT10001hr

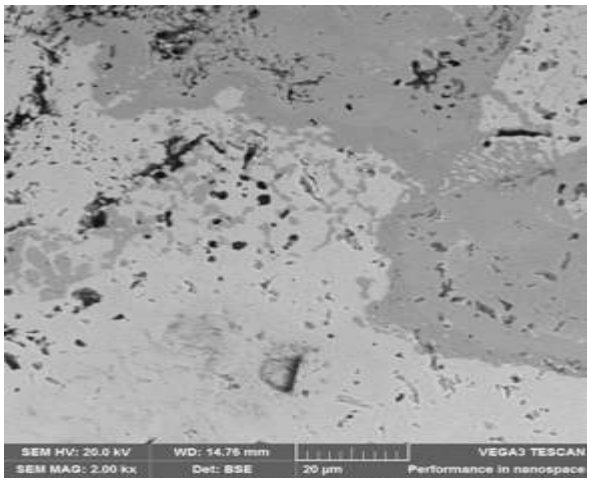

Figure 2c: SEM image of alloy HT10002hrs

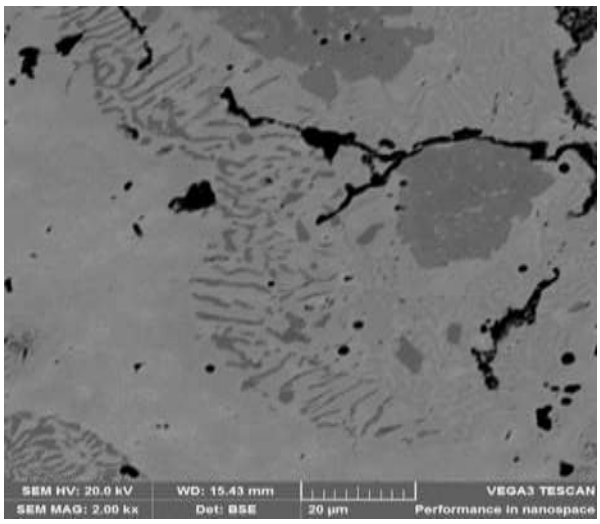

Figure 2d: SEM image of alloy HT8002hr

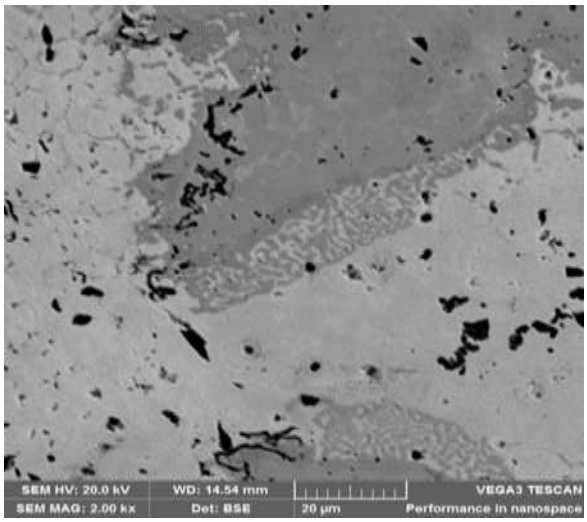

Figure 2e: SEM image of alloy HT8002hrs

The electrochemical potential of the alloy was investigated using H2SO4 solution. Table3 presents the corrosion data including the corrosion rate, while Fig 3(a) and 3(b) present results of the polarization tests. From the results obtained in Table 3 and Figure 3, the corrosion rate of the sample generally decreases after heat treatment. The untreated sample has the higher corrosion rate. This was attributed to the high anodic potential reached by the sample. Meanwhile, as the sample was heat treated there was decrease in corrosion rate. This may be attributed to the formation of a hard-thin film, which may have retarded the ingress of hydronium ions. As the heat treatment time decrease from 2 to 1 hr., the corrosion rate of the alloy decreased. Heat treatment contributes immensely to the corrosion behavior of the alloy (see Table3) E.g Corrosion rates of 8.058, 1.105, 1.66, 1.766 and 2.55mm/year were obtained for the untreated heat treated at 10000C for 1, 2hrs and 8000C for 1, 2hrs respectively. The various hard phases formed after heat treatments are the major factor responsible for the improvement in the corrosion behavior of this alloy.

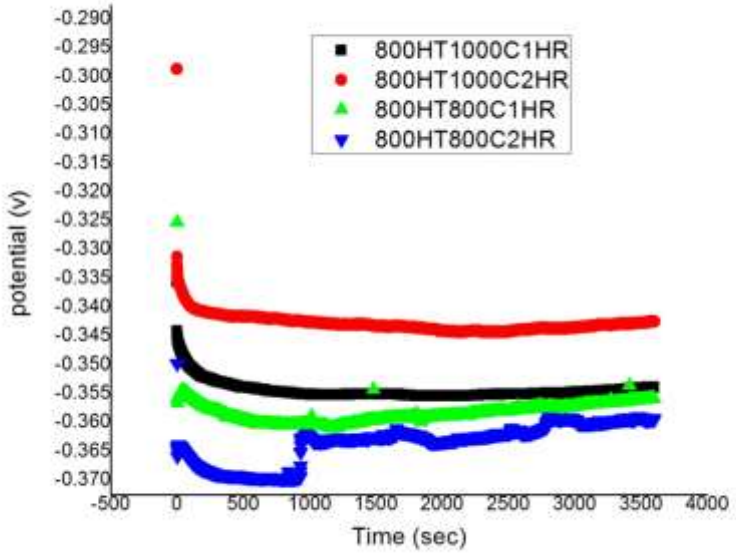

Figure 3a: Variation of open circuit potential with time

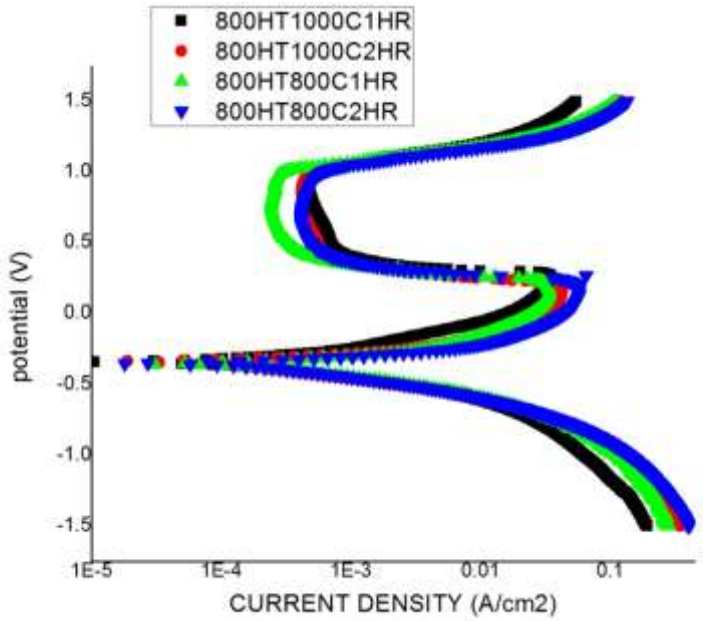

Figure 3b: potentiodynamic polarization curve

Table 3: Electrochemical corrosion data

SAMPLE	E_{corr}	I_{corr}(A/cm2)	R_p(Ω)	β_a (V/dec	β_c(V/dec)	CR (mm/Y)
CONTROL	-0.330	7.976e	3.32	0.053	0.091	8.058E+0
800HT1000C1HR	-0.306	1.032E-4	2.869E+1	0.047	0.114	1.105E+0
800HT1000C2HRS	-0.350	1.554E-4	4.55E+1	0.083	0.151	1.66E+00
800HT800C1HR	-0.353	1.6498E-4	2.012E+1	0.058	0.103	1.766E+0
800HT800C2HRS	-0.350	2.572E-4	2.06E+1	0.079	0.122	2.55E+0

Table 4: Upper and lower levels used and their responses

S/No	Temperatures (A) °c	Time (B) hrs	Corrosion rate (mm/yr)
1	800	2	0.255
2	800	1	0.1766
3	1000	2	0.166
4	1000	1	0.1105

The heat-treated sample may act as a cathode, which prevents conductance of ions but allows electronic conductance to some extent. It should also be emphasized that the electrical potential in all the samples decreases in the direction from the anode to the cathode (positive ions move towards the cathode, negative ions towards the anode (see Figures 3a). The surface of the anode in reality is much smaller than that of the cathode; i.e. the electrolytic current density is much higher near the anode. It is worthy to note in this present work that heat treatment temperature and time play a vital role in the electrochemical potential of all the samples. The sample that was heat treated at 1000°c for 1hour gave the optimum condition that led to the higher corrosion resistance. This optimum condition gave a protection efficiency of 86.29%.

Two factors and level of factorial design experiment were used to study the influences of heat treatment temperature and time on the corrosion behavior of the materials. Table 4, shows the upper and lower level s of each variable with their response values. Figure 4, shows the estimated response surface for the samples. it is observed that the corrosion rate increases with increase in heat treatment temperature and time. for example, as the temperature increases from 800 to 10000C and time. From 1 to 2hours the corrosion rate increased rapidly (see figure 4). Equation 1 shows the dependence of corrosion rate (C.R) on temperature and time.

Corrosion rate

C.R= +1.77025-0.38775* TEMPREATURE +0.33475*Time (1)

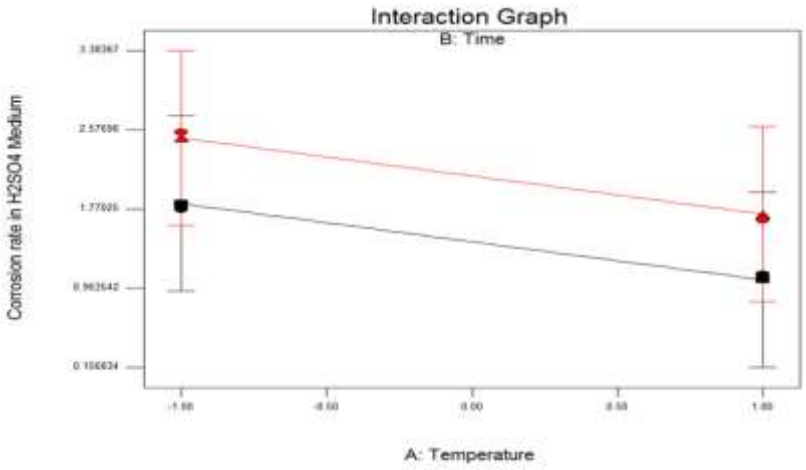

Figure 4a: Interaction curve for the corrosion behavior

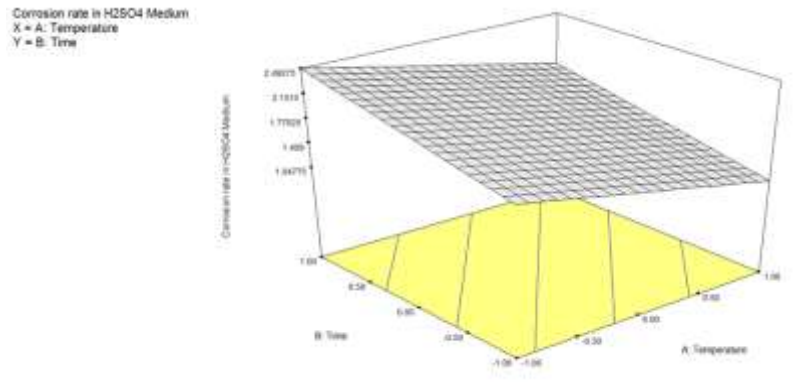

Figure 4b: 3-D plot for the corrosion behavior of the 800H alloy

From equation 1, it can be clearly seen that the coefficients associated with temperature and time are positive. It indicates that as the temperature rises from 800 to 10000C, the corrosion rate rises by 0.38775. Also, as the time increases from 1 to 2hours the corrosion rate rises by 0. 33475.This further supports the earlier observation in figure 4a and 4b.
Analysis of variance (ANOVA) was used to determine the design parameters significantly influencing the corrosion rate. Table 5 shows the results of ANOVA at 95% confidence level (significant level of $\propto$=0.05). The last column of table 5 shows the contribution (p) of each parameter to the response, indicating the degree of influence on the results.
The "Model F-value" of 40.03 implies the model is not significant relative to the noise. There is a 11.11 % chance that a "Model F-value" this large could occur due to noise.
Values of "Prob > F" less than 0.0500 indicate model terms are significant. In this case there are no significant model terms. Values greater than 0.1000 indicate the model terms are not significant. If there are many insignificant model terms (not counting those required to support hierarchy), model reduction may improve your model.

The "Pred R-Squared" of 0.8026 is in reasonable agreement with the "Adj R-Squared" of 0.9630.

Table 5: ANOVA for selected factorial model

Source	Sum of squares	DF	Mean square	F value	P value
Model	1.05	2	0.52	40.03	0.1111
A	0.60	1	0.60	45.87	0.0933
B	0.45	1	0.45	34.19	0.1078
Residual	0.013	1	0.013		
Cor Total	1.06	3			

Conclusion

From the results and discussion above the following conclusions can be made:

1. The heat-treated alloy shows better corrosion resistance than the untreated alloy.
2. Heat treatment temperature and time have great influence on the corrosion behavior and morphology of the alloy.
3. The sample heat treated at 1000OC for 1 hour gave a high protection efficiency of 86.29%
4. It has been established that heat treatment can be used in improving the corrosion resistance of the alloy.

References

Wlodek, S.T.; Kelly, M.; Alden D. (1992). The Structure of N18 Superalloys 1992. TMS, Warrendale, PA, U.S.A (S.D. Antolovich et al., eds), 467-476

Soucail, M.; Marty, M.; Octor, H. (1996). Development of Coarse Gran Structures in a Powder Metallurgy Nickel Base Superalloy N18. *Scripta Mater,* 34 (4), 519-525

Khadiah M. Emran (2015). Effects of concentration and temperature on the corrosion properties of the Fe-Ni-Mn alloy in HCL solutions. *Res Chem Intermed*, 41, 3583-3596

Viswanathan, G.B.; Sarosi, P.M.; Henry, M.F; Whitis, D.D.; Milligan, W.W.; Mills, M.J. (2005). Investigation of Creep Deformation Mechanisms at Intermediate Temperatures in Rene 88 DT. *Acta Mater,* 53, 3041-3057.

Locq, D.; Walder, A.; Marty, M.; Caron, P. (2000). Development of New PM Superalloys for High Temperature Application. *EUROMAT, Intermetallics and Superalloys,* 10, WILEY-VCH Verlag Gmbh, Weinheim, Germany (D.G. Morris et al., eds), 52-57

Wesley, W.A. and Copson, H.R. (1949). Effect of Non-Condensable Gases on Corrosion of Nickel in Steam Condensate. *TRANS. ELECTROCHEM*. SOC.,May,

Singh, Harminder and Sidhu, T.S. (2013). High Temperature Corrosion Behaviour of Ni-based Superalloy Superni-75 in the Real Service Environment of Medical Waste Incinerator. *Oxidation of Metals,* 80(5-6), 651-668

Dehmolaei, R., Shamanian, M. and Kermanpur A. (2009). Microstructural Changes and Mechanical Properties of Incoloy 800 after 15 years' service. *Materials Characterization* (60), 246-250.

Paula Rojas, Rosa Vera, Carola Martinez, Maria Villaroel (2016). Effect of the Powder Metallurgy manufacture Process on the Electrochemical Behaviour of Copper, Nickel and Copper Nickel Alloys in Hydrochloric Acid. *Int. J. Electrochem. Sci.,* 11, 4701-4711